VIII International Conference on Fracture Mechanics of Concrete and Concrete Structures
FraMCoS-8
J.G.M. Van Mier, G. Ruiz, C. Andrade, R.C. Yu and X.X. Zhang (Eds)

THE EFFECT OF CONCRETE STRENGTH ON CRACKING OF SFRC MEMBERS

G. TIBERTI[*], F. MINELLI[*], G.A. PLIZZARI[*] AND F.J. VECCHIO[†]

[*] University of Brescia
43, Via Branze, Brescia 25123, Italy
giuseppe.tiberti@ing.unibs.it; fausto.minelli@ing.unibs.it; giovanni.plizzari@ing.unibs.it
www.unibs.it

[†] University of Toronto
Department of Civil Engineering
35 St. George Street, Toronto, ON M5S 1A4, Canada
fjv@civ.utoronto.ca
www.civil.engineering.utoronto.ca

Key words: fibre reinforced concrete, reinforced concrete, steel fibre; crack widths; crack spacing; tension stiffening.

Abstract: Tension stiffening is still a matter of discussion into the scientific community. The study of this phenomenon is also relevant in structural members made of fibre reinforced concrete. This paper aims at investigating tension stiffening by presenting tension-test results on reinforced concrete prisms having different sizes, reinforcement ratios, amount of fibres and concrete strength. The influence of fibres in determining a more distributed crack patterns, characterized by narrower and more closely cracks, will be discussed. It is worth noticing that the expected smaller crack widths in addition to a low concrete porosity (which strictly depends on the water/cement ratio) is of paramount importance for enhancing structural durability.

1 INTRODUCTION

The use of Fibre Reinforced Concrete (FRC) has gained considerable attention in recent years, as demonstrated by its recent inclusion in the new fib Model Code 2010 [1] and by many international committees [2] or conferences [3, 4].

FRC has been particularly used in structural elements when crack propagation control is of primary importance, such as in slab-on-grade applications, precast tunnel segments or in beams where little or no shear reinforcement is provided. In several of these structural applications, the total amount of reinforcement consists of a combination of conventional rebars and fibres. Nowadays, the crack control of these fibrous RC elements is of paramount importance in order to guarantee the fulfilment of a key-parameter: durability. In fact, several codes require that structures have a defined service life during which the structural performance must satisfy minimum requirements by scheduling only ordinary maintenance.

Durability can be associated to permeability, defined as the movement of fluid through a porous medium under an applied pressure load, which is considered one of the most important property of concrete [5]. Permeability of concrete is strictly related to the material porosity but also to cracking. The former is basically controlled by the water/cement (w/c) ratio as well as by the degree of hydration and compaction. Concerning the latter, concrete should have an enhanced toughness to contrast cracking phenomena, which is generally provided by

structural fibres added to the concrete matrix.

The durability issue will be herein considered by focusing the attention on cracking in ordinary RC or FRC elements under uniform tension (tension tie specimens).

The deformation of a rebar embedded in concrete is significantly influenced by the bond between the two materials. In fact, it is well known that, after cracking, bond transfers tensile stresses from the rebar to the surrounding concrete (between cracks) that stiffen the response of a RC member subjected to tension; this stiffening effect is referred to as "tension stiffening". Several Authors studied this mechanism in traditional RC elements [6, 7].

In fibrous RC elements, an additional significant mechanism influences the transmission of tensile stresses across cracks arising from the bridging effect of the fibres. It clearly turns out that the combination of these two mechanisms (tension stiffening and the post-cracking residual strength provided by fibres at any crack) results in a different crack pattern, namely both the crack spacing and crack width. The collapse mode and the ductility of the elements may also be affected by stress concentrations due to optimized bond and the residual tensile stress at a crack.

Many preliminary studies have been carried out so far. Mitchell [8] presented one of the first studies for clarifying the beneficial effect of fibres in determining narrower and closely spaced cracks, as well as in mitigating the splitting cracks in the end regions while having low concrete covers. Bischoff ([9, 10]) performed monotonic and cyclic tension-stiffening tests and included shrinkage effects in the analysis. Noghabai [11] proposed an analytical model which describes the behaviour of tie-elements based on the observation of experimental tests.

The present paper describes a number of experimental results from a collaborative research program developed by the University of Brescia (Italy) and the University of Toronto (Canada), aimed at studying crack formation and development in FRC structures. Tension stiffening tests were carried out by varying the concrete strength, the reinforcement ratio, the fibre volume fraction and the fibre geometry. Brescia tested and interpreted tension members made of Normal Strength Concrete (NSC) while researchers at the University of Toronto tested identical members made of High Strength Concrete (HSC; with a concrete strength around 60 MPa and higher). A total of 59 uniaxial tension HSC specimens were tested at the University of Toronto (Canada), in addition to numerous material tests to quantify the behaviour of the concretes used in the different test series. Complete details of the experimental program and the full experimental results are provided by Deluce [12]. A total of 109 tests were done at the University of Brescia on NSC; details of this experiments are reported in [13] and [14].

This paper is mainly focuses on the effect of concrete strength on the behaviour exhibited by the specimens in terms of crack formation and development.

2 EXPERIMENTAL INVESTIGATION

The experimental program was designed so that a comprehensive database of uniaxial tension tests of reinforced concrete RC and SFRC members with conventional steel rebars (one bar in the centre of the specimen) could be generated. These fibrous and non-fibrous members will be identified as SFRC and RC tensile ties, respectively. NSC/HSC will be used to underline the different concrete strength.

The following key-parameters were investigated:

- Concrete cylinder compressive strength: from 25 MPa to 95 MPa;
- Square element size: from 50 to 200 mm;
- Clear concrete cover: from 20 to 85 mm;
- Effective reinforcing ratio: from 0.98 to 4.17%;
- ϕ/ρ_{eff} ratio: from 271 mm to 2042 mm;
- Bar diameter: from 10 to 30 mm;
- Specimen length: from 950 mm to 1500 mm;
- Volume fraction of fibres: from 0 to 1.5%.

2.1 Uniaxial Tension RC and SFRC Test Specimen Configurations

In a first phase of research, 64 prismatic tensile members containing conventional steel reinforcing rebars having the geometry shown in Figure 1a were cast with NSC at the University of Brescia. Each specimen was 950 mm long and have a square cross section; five sides were selected (50, 80, 100, 150 and 200 mm). Reinforcing bars having a diameter of 10, 20 and 30 mm (B450C steel, according to EN 10080, [15]), corresponding to a reinforcement ratio (ρ) varying from 1.24% to 3.24%, have been used throughout this first phase. At the University of Toronto, 59 members of HSC, having the same cross-sections and a length equal to 1000 mm, were cast and tested. The deformed steel reinforcing bar sizes varied from 10M to 30M (Canadian bar sizes, [16]). Consequently, for HSC tensile ties, the reinforcement ratio (ρ) ranged from 1.35% to 4.17%. The properties of the reinforcing bars used in NSC and HSC tie elements are reported in Table 1.

A second phase of research was developed only at the University of Brescia in order to better investigate the behaviour of NSC tensile members. With this purpose, further 45 prismatic ties were cast and tested; reinforcing bars having the same diameter were used, whereas four square cross sections were selected (80, 120, 180 and 200 mm size) and a reinforcement ratio ρ from 0.98% to 2.23% was adopted. The specimens having a rebar diameter equal to 20 and 30 mm were longer with respect to those of the previous phase (1500 mm vs. 950 mm). In fact, since the number of cracks expected was higher, the average crack spacing could be better evaluated. Members with a rebar diameter equal to 10 mm were 1000 mm long. Geometry and reinforcement details of specimens of this second phase are depicted in Figure 1b.

Different dosages and types of steel fibres were included into the NSC matrix: both macro and micro fibres were adopted with a total volume fraction up to 1.0%. The micro fibres were only used in addition to macro fibres determining a hybrid system that can help both early cracking (mainly controlled by micro fibres) and final macro-cracking (mainly controlled by macro fibres).Referring to HSC elements, three types of hooked-end macro steel fibres were used, with volume fractions up to 1.5%.

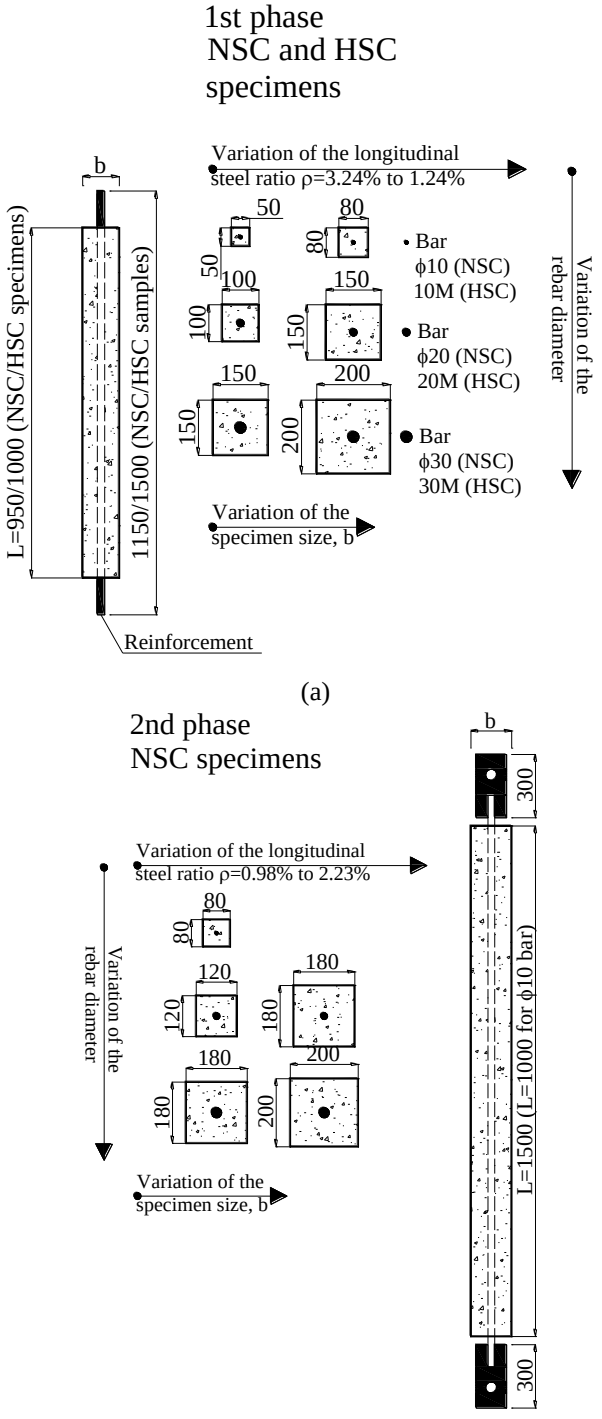

Figure 1: Geometry and reinforcement details of specimens (1st (a) and 2nd (b) phase).

Based on the different combinations of concrete strength and fibrous reinforcement, a total of 14 test series were cast and tested, as summarized in Table 2. Referring to HSC elements (first phase) the experimental program includes one non-fibrous control series (PC) and five series containing steel fibres. For NSC elements, two plain control (PC) series and six SFRC series were globally tested (first and second phase). For each series, Table 2 reports the material identification (batch ID), the volume fraction of steel fibres used and fibre designation. Note that the designation used for each fibre type denotes the fibre length as the first number and the fibre diameter as the second. Table 3 summarizes the main characteristics of all 5 fibre typologies.

Each combination of fibre reinforcement, member dimension and steel reinforcement ratio defines a specific set of tests, whose repetitions and notations are listed in Table 4.

Table 1: Properties of steel reinforcing bars.

	Rebar	**A_s (mm^2)**	**d_b (mm)**	**E_s (GPa)**	**f_y (MPa)**	**ε_{sh} ($x10^{-3}$)**	**f_{ult} (MPa)**	**ε_{ult} ($x10^{-3}$)**
Rebars used in NSC specimens	ϕ10	78	10	198	522	29.7	624	-
	ϕ20	314	20	198	515	20.2	605	-
	ϕ30-1†	707	30	187	554	15.8	672	-
	ϕ30-2†	707	30	182	484	17.9	604	-
Rebars used in HSC specimens	10M	100	11.3	199	442	27.0	564	164.0
	20M-1†	300	19.5	194	456	21.2	592	144.2
	20M-2†	300	19.5	188	525	17.3	653	111.6
	30M	700	29.9	187	376	11.0	558	177.0
† - The 20M and ϕ30 bars came from two different production heats								

Table 2: Mechanical properties of concrete and fibre contents.

		Batch ID	f_{cm} [MPa]	f_{ctm} [MPa]	Volume Fraction of Steel Fibres V_f $[\%]_{vol.}$					
					Fibres 30/0.62	Fibres 13/0.20	Fibres 30/0.38	Fibres 30/0.55	Fibres 50/1.05	$V_{f,tot}$
1st phase	NSC	0 Plain	40.5	3.71	-	-	-	-	-	-
		0.5M	39.7	3.37	0.5	-	-	-	-	0.5
		1M	25.4	2.60	1	-	-	-	-	1
		1M†	36.4	3.50	1	-	-	-	-	1
		1M+m	43.3	2.81	0.5	0.5	-	-	-	1
	HSC	Plain	91.4	4.93	-	-	-	-	-	-
		FRC1	75.7	4.55	-	-	0.5	-	-	0.5
		FRC2	52.8	3.94	-	-	1	-	-	1
		FRC3	56.8	3.96	-	-	1.5	-	-	1.5
		FRC4	41.7	3.28	-	-	-	1.5	-	1.5
		FRC5	75.0	4.54	-	-	-	-	1.5	1.5
2nd phase	NSC	0 Plain	47.2	3.50	-	-	-	-	-	-
		0.5M	40.8	3.35	0.5	-	-	-	-	0.5
		1M	27.4	2.85	1	-	-	-	-	1
† - The series 1M was repeated										

Table 3: Characteristics of fibres employed.

Fibre ID	Type of steel	Shape	f_{uf} [MPa]	l_f [mm]	ϕ_f [mm]	l_f/ϕ_f [-]	Batch ID
30/0.62	Carbon	Hooked-end	1270	30	0.62	48.39	0.5M, 1M, 1M†, 1M+m
13/0.20	High carbon	Straight	2000	13	0.20	65.0	1M+m
30/0.38	High carbon	Hooked-end	2300	30	0.38	78.95	FRC1, FRC2, FRC3
30/0.55	Carbon	Hooked-end	1100	30	0.55	54.55	FRC4
50/1.05	Carbon	Hooked-end	1100	50	1.05	47.62	FRC5

Table 4: Experimental program and specimen notation.

Phase		Rebar	Batch ID	b [mm]	Length, L [mm]	Reinf. Ratio (%)	Clean cover [mm]	Specimen ID
1st phase	NSC	ϕ10	0 Plain	50	950	3.24	20	N 50/10 – 0
			0.5M					N 50/10 – 0.5M
			1M					N 50/10 – 1M
			1M†					N 50/10 - 1M†
			1M+m					N 50/10 - 1M+m
		ϕ10	0 Plain	80	950	1.24	35	N 80/10 – 0
			0.5M					N 80/10 – 0.5M
			1M					N 80/10 – 1M
			1M†					N 80/10 - 1M†
			1M+m					N 80/10 - 1M+m
		ϕ20	0 Plain	100	950	3.24	40	N 100/20 - 0
			0.5M					N 100/20 – 0.5M
			1M					N 100/20 – 1M
			1M†					N 100/20 – 1M†
			1M+m					N 100/20 - 1M+m
		ϕ20	0 Plain	150	950	1.41	65	N 150/20 – 0
			0.5M					N 150/20 – 0.5M
			1M					N 150/20 – 1M
			1M†					N 150/20 – 1M†
			1M+m					N 150/20 - 1M+m
		ϕ30	0 Plain	150	950	3.24	60	N 150/30 – 0
		ϕ30	0 Plain	200	950	1.80	85	N 200/30 – 0
	HSC	M10	0 Plain	50	1000	4.17	19.35	H 50/10 – 0
			FRC1					H 50/10 – FRC1
			FRC2					H 50/10 – FRC2
			FRC3					H 50/10 – FRC3
			FRC4					H 50/10 – FRC4
			FRC5					H 50/10 – FRC5
		M10	0 Plain	80	1000	1.59	34.35	H 80/10 – 0
			FRC1					H 80/10 – FRC1
			FRC2					H 80/10 – FRC2
			FRC3					H 80/10 – FRC3
			FRC4					H 80/10 – FRC4
			FRC5					H 80/10 – FRC5
		M20	0 Plain	100	1000	3.09	40.25	H 100/20 – 0
			FRC1					H 100/20 – FRC1
			FRC2					H 100/20 – FRC2
			FRC3					H 100/20 – FRC3
			FRC4					H 100/20 – FRC4
			FRC5					H 100/20 – FRC5
		M20	0 Plain	150	1000	1.35	65.25	H 150/20 – 0
			FRC1					H 150/20 – FRC1
			FRC2					H 150/20 – FRC2
			FRC3					H 150/20 – FRC3
			FRC4					H 150/20 – FRC4
			FRC5					H 150/20 – FRC5
		M30	0 Plain	150	1000	3.21	60.05	H 150/30 – 0
			FRC1					H 150/30 – FRC1
			FRC2					H 150/30 – FRC2
			FRC3					H 150/30 – FRC3
			FRC4					H 150/30 – FRC4
			FRC5					H 150/30 – FRC5

Phase		Rebar	Batch ID	b [mm]	Length, L [mm]	Reinf. Ratio (%)	Clean cover [mm]	Specimen ID
		M30	0 Plain	200	1000	1.78	85.05	H 200/30 – 0
			FRC1					H 200/30 – FRC1
			FRC2					H 200/30 – FRC2
			FRC3					H 200/30 – FRC3
			FRC4					H 200/30 – FRC4
			FRC5					H 200/30 – FRC5
2nd phase	NSC	ϕ10	0	80	1000	1.24	35	N 80/10 – 0
			0.5%					N 80/10 – 0.5M
			1.0%					N 80/10 – 1M
		ϕ20	0	120	1500	2.23	50	N 120/20 – 0
			0.5%					N 120/20 – 0.5M
			1.0%					N 120/20 – 1M
		ϕ20	0	180	1500	0.98	80	N 180/20 – 0
			0.5%					N 180/20 – 0.5M
			1.0%					N 180/20 – 1M
		ϕ30	0	180	1500	2.23	75	N 180/30 – 0
			0.5%					N 180/30 – 0.5M
			1.0%					N 180/30 – 1M
		ϕ30	0	200	1500	1.80	85	N 200/30 – 0
			0.5%					N 200/30 – 0.5M
			1.0%					N 200/30 – 1M

Table 5: Fracture parameters of the FRCs according to EN 14651 (mean values).

		Batch ID	Fracture parameters of the SFRCs according to EN-14651				
			f_{Lm} [MPa]	f_{R1m} [MPa]	f_{R2m} [MPa]	f_{R3m} [MPa]	f_{R4m} [MPa]
1st phase	NSC	0.5M	5.46	5.00	4.55	4.05	3.46
		1M	4.91	5.79	5.15	4.40	3.75
		1M†	4.81	5.09	4.12	3.42	3.01
		1M+m	5.97	6.30	5.35	4.35	3.54
	HSC	FRC1	6.11	8.98	7.82	6.74	5.54
		FRC2	4.94	10.08	9.53	8.79	7.51
		FRC3	4.98	7.38	7.32	6.60	5.50
		FRC4	4.63	6.71	5.6	4.24	3.75
		FRC5	5.23	7.66	6.91	6.03	4.79
2nd phase	NSC	0.5M	4.60	4.12	4.07	3.35	2.69
		1M	4.64	5.43	4.89	4.36	3.86
† - The series 1M was repeated							

2.2 Material Tests

A number of material tests were carried out in order to evaluate the material properties of the concretes used in the RC and SFRC specimens.

Regarding NSC series, standard tests on 150 mm side cubes were carried out. The tensile strength (direct tension test) was measured from ϕ 80·210 mm (first phase) and ϕ 150·300 mm cylinders (second phase).

Referring to HSC series, standard tests on 150 mm · 300 mm concrete cylinders were carried out to measure the compressive strength of the material.

Table 2 reports the main values of cylinder compressive and tensile strength for the 14 materials tested.

In addition, all SFRCs were mechanically characterized according to the European Standard EN 14651 [17], which requires that three point bending tests (3PBT) to be performed on small notched beams (150·150·550 mm). Based on experimental curves concerning the total nominal stress vs. Crack Mouth Opening Displacement (CMOD), the post-cracking residual strengths

f_{Ri} (for 4 different values of CMOD, i.e. 0.5, 1.5, 2.5 and 3.5 mm), and the flexural tensile strength (limit of proportionality) f_L, were calculated and are listed in Table 5.

2.3 Set-up and instrumentation

In the first phase of research, tensile tests (both, NSC and HSC series) were performed by means of hydraulic servo-controlled (closed-loop) testing machines. Tests were carried out under stroke control (by clamping both the rebar ends) by monitoring the specimen behaviour up to the onset of the strain-hardening branch of the rebar. The deformation rate up the yield limit of the steel was varied from 0.1 to 0.2 mm/min. At yielding, the rate was progressively increased from 0.5 mm/min up to 1 mm/min, the latter at an average strain of approximately 2%.

Four Linear Variable Differential Transformers (LVDTs, one for each side), were placed to measure the deformation of the specimen over a length ranging from 900 mm to 950 mm.

Regarding NSC elements, all specimens made of plain concrete and SFRC series 1M[†] were stored in a fog room (R.H. > 95%; T=20 ± 2°C) until 2 or 3 days before testing; then, they were air dried in the laboratory. All the other specimens were moist cured with wet burlap under plastic sheet until 2 or 3 days before testing, since it was not possible, for space restriction, using the same fog room. For these specimens, shrinkage effects were not probably totally controlled, even though the member response could be corrected by taking into account the effect of the initial shrinkage strain [18]; however, shrinkage does not significantly influence the final crack pattern and crack spacing. Referring to HSC elements, free shrinkage prism tests were carried out in order to estimate the restrained shrinkage within the RC and SFRC specimens. In the tensile tie tests, restrained shrinkage effects were significant since both the free shrinkage strains and reinforcement ratios were quite high. From the free shrinkage strains, the shrinkage-induced offset strain was calculated, as suggested by [18].

In the second phase, the experimental program was carried out only at the University of Brescia on NSC tie elements, by means of an available steel reacting frame conveniently modified. Two steel plates, previously holed, were welded at the ends of the specimen (see Figure 1b), which was connected by pins to the reacting rig (Figure 2). The tests were carried out under stroke control and by assuming the same load-procedure previously described for the first phase. Four LVDTs, one for each side of the sample, were placed to measure the deformation of the specimen over a length of 1400 mm (members with a bar diameter of 20 and 30 mm) and 900 mm (bar diameter of 10 mm). All specimens were stored in a fog room (R.H. > 95%; T=20 ± 2°C) until 2 or 3 days before testing; then they were air dried in the laboratory. In the fog room shrinkage strains were measured by means of free shrinkage prisms. Since the measured strains were negligible, no-shrinkage offset strains were applied in the analysis of tensile members tested in the second phase.

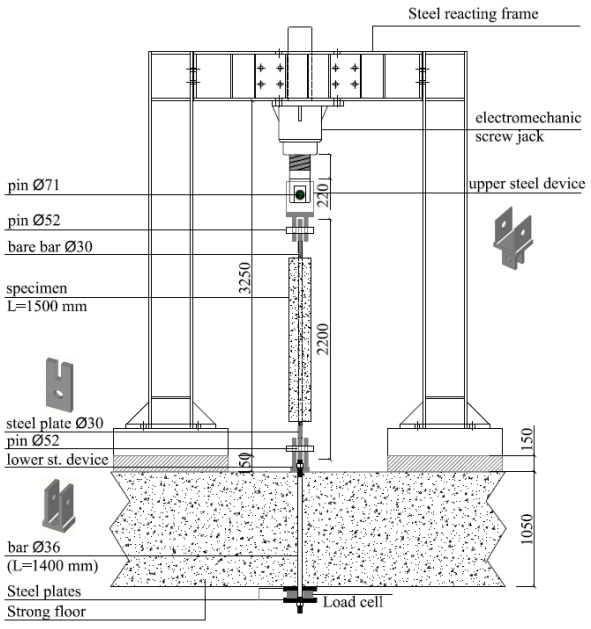

Figure 2: Specimen 1500 mm long placed in the centre of the steel reacting frame. Notice the details of the holed steel plates (measures given in mm).

3 RESULTS AND DISCUSSION

3.1 Typical Tensile Tie behaviour

The diagrams reported in Figure 3a and in Figure 3b evidence the typical response in terms of axial load vs. average tensile strain of RC and SFRC for NSC and HSC series, respectively. The average member strain was calculated as the mean elongation of the 4 LVDTs, divided by the length of the base measurement. In both diagrams, a comparison between one typical plain and corresponding SFRC member is proposed. Also, the response of the corresponding bare bars is reported.

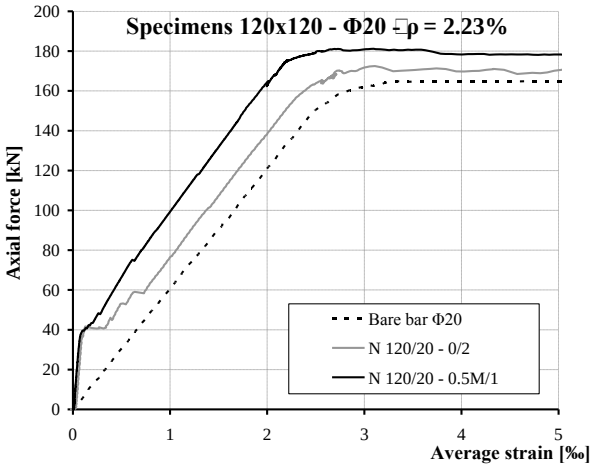

(a)

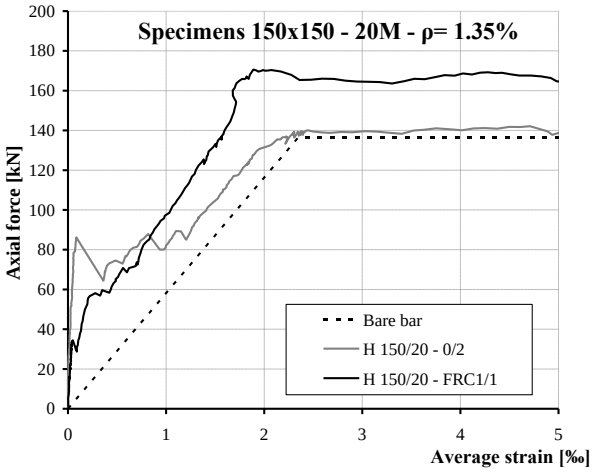

(b)

Figure 3: Typical response of non-fibrous reference Series of NSC (a) and HSC (b).

The results are plotted up to a maximum average strain of $5 \cdot 10^{-3}$, in order to properly describe the behaviour at Serviceability Limit State (SLS, where the crack and displacement control is of main importance), and also in order to assess the behaviour at yielding.

In RC specimens, the elastic stiffness remained relatively high until the initial crack occurred, point at which tension stiffening initiated and the overall stiffness significantly reduced. Since no fibres were included, the transmission of any residual stress across cracks was not possible, and so the load-deformation response quickly approached that of the bare bar and the maximum load was limited by the yield strength of the rebar.

In a typical SFRC specimen, the uncracked response was similar to that of a non-fibrous specimen, as expected. After cracking, fibres provided a noticeable increment of the concrete toughness, guaranteeing a considerable residual strength through cracks (this phenomenon is defined as tension softening or hardening). Accordingly, by referring to a certain average member strain, the improved toughness of SFRC determined an increment of the average tensile strength of the undamaged concrete portions between two consecutive cracks. As a result, in both NSC and HSC tie elements, the tension-stiffening behaviour of SFRC series was more pronounced than that of RC specimens. In addition, after the first cracking, the reduction in load-carrying capacity was significantly more gradual for SFRC members than in RC specimens. The improvement of the tension-stiffening can be clearly evidenced in the stabilized crack stage for NSC fibrous elements (Figure 3a) whereas it is relevant, in the HSC ties, only for average strains greater than $1 \cdot 10^{-3}$. (Figure 3b). The main reason is that SFRC elements plotted in Figure 3b experienced particularly large shrinkage strains; this caused the apparent cracking load to decrease with respect to that of a RC specimen which, on the contrary, exhibited lower shrinkage.

By analyzing the typical responses of SFRC tie elements (Figure 3a/b), the fibre resistant contribution (post-cracking strength) can be clearly shown at yielding since SFRC toughness allows for a transfer of residual tensile stresses between the crack faces, with a consequent increase of the bearing capacity of

the structural member, whereas in the control samples (plain) there is no possibility of increasing the ultimate capacity after yielding. It is worthwhile mentioning that some splitting cracks were detected in both RC and SFRC specimens; however these cracks have little effects on the tensile behaviour of the specimens.

3.2 Crack formation and development

A significant aspect herein investigated concerns the crack pattern and its evolution in terms of mean crack spacing.

The mean crack spacing of a single specimen was evaluated by measuring the distance between visible cracks on the surface. Furthermore, the mean crack spacing of each set of samples was calculated as the mean values of the measured mean values on each single specimen. This approach is reliable since no crack-localizations occurred in the sample before the yielding point.

In Figure 4a and b, the evolution of the mean crack spacing (s_{rm}) has been plotted as a function to the average strain up to the end of the crack formation stage, for specimens N 200/30 and H 200/30, respectively. Note that in HSC specimens, the effect of shrinkage was computed according to [12]. The diagrams are plotted for the different SFRC under investigation in order to evidence the influence of fibre content on the cracking behaviour. With this purpose, for HSC tie elements (Figure 4b), the curves are referred to series FRC1, FRC2, FRC3 (corresponding to fibres 30/0.38 and a volume fraction of 0.5%,1%, 1.5%, respectively, see Table 2). On the other hand, the NSC series (Figure 4a) are plotted for macro fibre (30/0.62) and two dosages: V_f=0.5% and 1% (for specimens tested in the second phase). The responses of control series are also plotted as a reference.

By referring to a certain member average strain, it is demonstrated that as the fibre content increases, the mean crack spacing decreases. This tendency is consistent for any given average strain and it also applies, as expected, at the end of the crack formation stage, where the stabilized crack stage begins, as well depicted in the two graphs by the horizontal asymptotes, corresponding to the final mean crack spacing. In fact, the residual post-cracking strength provided by steel fibres contributes to the reduction of the transmission length necessary to transfer tensile stresses in concrete by means of bond; hence, the mean crack spacing and the corresponding mean crack width will diminish.

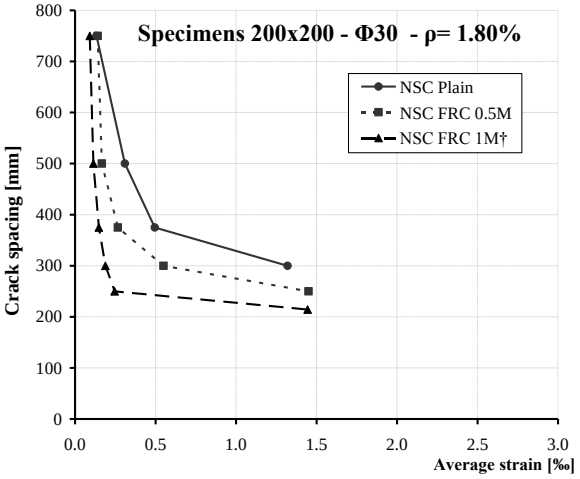

(a)

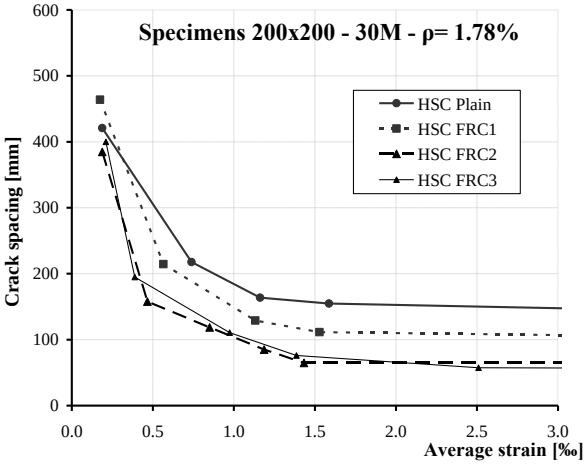

(b)

Figure 4: Evolution of the mean crack spacing of fibrous non-fibrous Series NSC (a), HSC (b)

The analysis of the evolution of the mean crack spacing with respect to the average member strain (for all the series investigated) has demonstrated that the crack formation stage of NSC fibrous and non-fibrous specimens corresponds approximately to a range of strains varying from 0.5 to $1.5 \cdot 10^{-3}$; a similar tendency can be reported for HSC tie elements, even though the range of strain is slightly higher. In particular, according to the

enhanced fibre resistant contribution, one would expect a lower value of the average strain corresponding to the end of the crack formation stage. A clear tendency was not observed.

In order to better evaluate the effect of concrete strength on the cracking process, the crack pattern evolution of the previously described N 200/30 and H 200/30 specimens (Figure 4) has been compared in Figure 5. Both RC and SFRC tie elements (the latter reinforced by macro fibres), with V_f of 0.5% and 1%, are plotted. Note that the comparison of SFRC series depends not only on the concrete strength but it is also rather influenced, referring to the same fibre content, by the fibre toughness. Referring to Figure 5, the NSC specimens contain fibres 30/0.62 whereas HSC samples contain fibres 30/0.38 (see Table 5 for details).

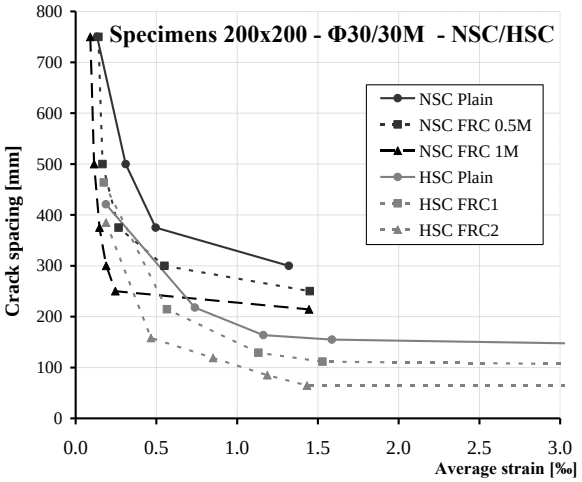

Figure 5: Comparison of the evolution of the mean crack spacing: NSC vs. HSC.

The diagrams plotted in Figure 5 clearly evidence that, referring to the same longitudinal reinforcement ratio (conventional rebar) and the same clear concrete cover, RC HSC elements present a rather smaller mean crack spacing and, consequently, smaller crack widths with respect to corresponding NSC members. This tendency is consistent for average member strains ranging from the crack formation stage to the stabilized crack stage. The same trend can be also outlined for SFRC specimens, even though the rate of reduction of crack spacing should not only be attributed to concrete strength but also to the FRC toughness, as aforementioned.

Referring to the member average strain at the end of the crack formation stage, no significantly effects of the concrete strength on this parameter was observed.

In Figure 6 the mean crack spacing (s_{rm}) is plotted vs. the key parameter ϕ/ρ_{eff}, which is generally included in many building codes. In Figure 6a the experimental results are plotted with reference to RC members, whereas in Figure 6b the trend of SFRC members presenting a total $V_f \leq 1\%$ is reported (the results include macro fibres, macro+micro fibres according to all combinations presented in Table 4). Note that NSC corresponds to tie elements having a cylindrical concrete compressive strength lower than 50 MPa, whereas HSC refers to members with a higher value. The trend reported for RC elements (Figure 6a) confirms the tendency previously underlined in Figure 5: by referring to specimens having the same ϕ/ρ_{eff}, the use of HSC determines a considerable reduction of the mean crack spacing (with percentages up to 50%). Since several formulations proposed in literature or in design codes define the crack spacing linearly proportional to parameter ϕ/ρ_{eff}, it is meaningful evaluating the dispersion of results according to a linear regression. As depicted in Figure 6a, the coefficient of correlation R^2 is equal to 0.92 for the NSC control samples and 0.83 for HSC elements. Basically, a possible linear relationship between s_{rm} vs. ϕ/ρ_{eff} could be reliable, even though that should be a function of the concrete strength, differently from most of published relationships of s_{rm}.

The s_{rm} vs. ϕ/ρ_{eff} trend for SFRC ties, only for $V_f \leq 1\%$, as depicted in Figure 6b, is rather similar: a global reduction of the mean crack spacing with higher concrete strength is noticeable.

Furthermore, as expected, the crack spacing of the SFRC series are smaller than the corresponding RC due to the enhanced material toughness. The linear coefficient of correlation R^2 is 0.64 for both NSC and HSC SFRC elements, evidencing a poorer fitting. The reduction of the R^2 coefficient, with

respect to control samples, is probably due to the higher dispersion of the results in presence of fibres: in fact, for the sake of simplicity, different combinations of fibrous reinforcement (presenting diverse toughness ranges) are included in the comparison shown in Figure 6b. In other words, both the effect of concrete strength and toughness is embedded on that graph. A broader test database should be necessary to clearly identify the effect of each parameter on the crack spacing.

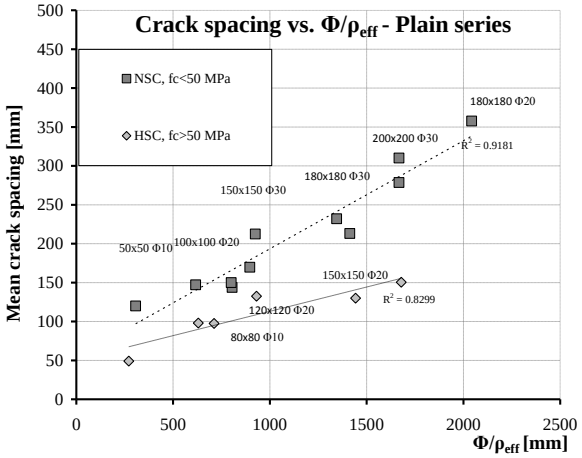

(a)

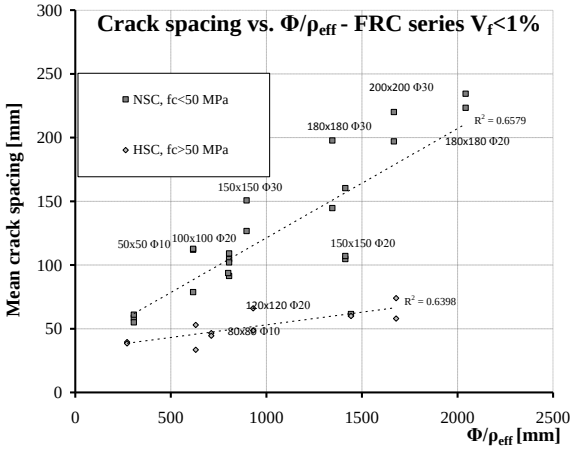

(b)

Figure 6: Crack spacing vs. ϕ/ρ_{eff} Non-fibrous Series (a) Fibrous Series (b).

4 CONCLUSIONS

In the present paper, a broad experimental study within a joint research program between the Universities of Brescia (Italy) and Toronto (Canada) is presented. A series of 109 NSC tie tests have been carried out in Brescia while Toronto tested a series of 59 members made of HSC.

Based on the results above mentioned, the following main conclusions might be drawn:

- the use of HSC determines a noticeable reduction of the mean crack spacing with respect to normal strength ones. This tendency was clearly evidenced for both plain and FRC specimens;

- the stabilized crack stage does not seem to be influenced either by the enhanced toughness (in FRC materials herein considered) and concrete class: in both the cases, a higher number of cracks form, without a clear indication that the crack stabilized stage develops later or earlier than in both NSC or non-fibrous elements.

- FRC diffusely influences the behaviour of tension-ties at SLS, by reducing crack width and determining a crack patterns with narrower and closely spaced cracks;

- FRC stiffens the post-cracking response of RC members and it is effective in diminishing the deflections of the structures. This is also a key-point for SLS design purposes.

Further studies have to be planned and performed for better understanding the relationship between FRC toughness and reinforcement ratio and for coming up with an analytical model in order to better predict the average crack spacing.

4 ACKNOWLEDGMENTS

A special acknowledgment goes to M.Sc. Eng. Giovanni Bocchi, Matteo Campanelli, Massimo Ferrari, Emanuele Maffetti, Ivan Pedrali, Matteo Romelli and Luca Schioppetti, to students Marco Franceschini and Daniel Sandoval Peña, and to the technician Mr. Andrea Delbarba for their valuable work in performing the tests and in the data processing. The Authors are also grateful to Alfa Acciai SpA (Brescia, Italy) for its valuable support in supplying all rebars for the experimental program.

REFERENCES

[1] Model Code 2010, “Final Complete Draft”, fib bulletins 65 and 66, March 2012-ISBN 978-2-88394-105-2 and April 2012-ISBN

978-2-88394-106-9.

[2] ACI Committee 544, "Design considerations for steel Fibre Reinforced Concrete", ACI 544.4R-88, American Concrete Institute, ACI Farmington Hills, MI (1999).

[3] Di Prisco, M., Felicetti, R., and Plizzari, G.A. (eds.), "Fibre-Reinforced Concrete", BEFIB 2004, Bagneux, France, RILEM Publications S.A.R.L., PRO39 (2004).

[4] Gettu, R. (ed.), "Fibre Reinforced Concrete: Design and Applications", BEFIB 2008, Bagneux, France, RILEM Publications S.A.R.L., PRO60 (2008).

[5] Banthia, N., and Bhargava, A., "Permeability of Stressed Concrete and role of Fibre Reinforcement", ACI Materials Journal, V. 104, No. 1, pp. 70-76 (2007).

[6] Beeby, A. W., "The prediction of Cracking in Reinforced Concrete Members", PhD Thesis, University of London (1971).

[7] Beeby, A. W., and Scott, R. H, "Cracking and deformation of axially reinforced members subjected to pure tension", Magazine of Concrete Research, 57, No.10, Dec., pp. 611-621 (2005).

[8] Mitchell, D., and Abrishami, H. H., "Influence of steel fibres on tension stiffening", ACI structural journal, No.93-S67, November-December, pp. 703-710 (1996).

[9] Bischoff, P.H., and Fields, K., "Tension stiffening and cracking of high strength reinforced concrete tension members", ACI structural journal, No. 101-S44, July-August, pp. 447-456 (2004).

[10] Bischoff, P.H., "Tension stiffening and cracking of steel fibre reinforced concrete", Journal of Material in Civil Engineering, V. 15, No.2, pp.174-182 (2003).

[11] Noghabai, K., "Effect of tension softening on the performance of concrete structures. Experimental, analytical and computational studies", Doctoral Thesis, Div. of Structural Engineering, Lulea University of Technology, 186 pp (1998).

[12] Deluce, J., 2011. Cracking Behaviour of Steel Fibre Reinforced Concrete Containing Conventional Steel Reinforcement., MASc Thesis. University of Toronto, 2011, pp. 506 [www.civ.utoronto.ca/vector/theses.html].

[13] Minelli, F., Tiberti, G., and Plizzari, G.A., "Crack Control in RC Elements with Fibre Reinforcement", ACI Special Publication ACI SP-280: Advances in FRC Durability and Field Applications CD-ROM, Vol. 280, Editors: Corina-Maria Aldea & Mahmut Ekenel, December 2011, pp. 18 (2011).

[14] Tiberti, G., Minelli, F. and Plizzari, G.A., "Crack control in fibrous RC Elements", in Proceedings of the eighth RILEM International Symposium (BEFIB 2012) "Fibre reinforced Concrete: challenges and opportunities, Editors: J.A.O Barros et al., September 19-21, 2012, pp. 187-188.

[15] EN 10080, Steel For The Reinforcement Of Concrete - Weldable Reinforcing Steel, 2005, pp. 25.

[16] CSA G30.18-09 - Carbon steel bars for concrete reinforcement, pp.32.

[17] EN 14651, "Test method for metallic fibre concrete - Measuring the flexural tensile strength (limit of proportionally (LOP), residual)", European Committee for Standardization, 18 pp (2005).

[18] Bischoff, P.H., 2001, "Effect of shrinkage on tension stiffening and cracking in reinforced concrete", Canadian Journal of Civil Engineering, V. 28, No.3, pp. 363-374.